Far Field Impacts of the Redirection of Siberian Rivers

S. G. Hartharn-Evans[1,2], T. Rippeth[2]

[1]School of Mathematics, Statistics and Physics, Newcastle University, NE1 7RU, UK

[2]School of Ocean Sciences, Bangor University, Bangor, LL59 5AB, UK

Key Points:

- Past proposal to divert Eurasian rivers away from the Arctic Ocean is investigated.
- The diversion would result in a reduction of upper ocean stratification.
- This reduction could potentially lead to increased ventilation of intermediate depth Atlantic water leading to enhanced sea ice melt.

Corresponding author: Samuel Hartharn-Evans, s.hartharn-evans2@ncl.ac.uk

Abstract

For over 150 years, plans to divert Arctic Ocean-draining rivers southwards in order to relieve an ongoing water supply crisis in central Asia have been discussed. Recent insights have identified the importance of freshwater in regulating the role of heat associated with intruding intermediate depth Atlantic water in driving Arctic Ocean sea ice decline. Here we assess the potential impact of the redirection of the Ob', Yenisey, Northern Dvina and Pechora rivers on upper ocean density structure, and by implication, the aerial sea ice extent. A simple 1D model is applied in which freshwater content of the upper ocean water column is reduced to mimic the diversion of the rivers, and the impact on water column stratification assessed. The results show that the impact is dependent on distribution of riverine freshwater in the upper water column. If the impact of reduced freshwater is spread through the entire water column, down to the Atlantic Water Layer, the level of stratification is reduced by an average of 28%, more than the seasonal variability in stratification. However, if the changes were limited to the surface layer, the resultant reduction in stratification is less, only 17%, but the direct entrainment of deeper, warmer waters is found to occur. At a time when climate change and population growth put increasing pressure on water resources, these results show the sensitivity of a region critical to global weather and climate to anthropogenic attempts to resolve water resource issues many thousands of kilometres away.

1 Introduction

Climate change and the demands of a growing global population are driving increased pressures on global water resources. A consequence has been the proposal of a number of major water diversion projects globally, such as the ongoing *South-North Water Transfer Project* in China. Such schemes may seem to provide a solution to regional water demands, but may also have unintended consequences. Here, we examine the potential far-field impact of recurring proposals which have been made to divert northward flowing Siberian rivers to the south. The purpose of the proposed diversion scheme is to tackle the geographical disparities of water supply and demand across the western-central Siberian region (e.g. Pearce, 2004; Shabad, 1983). Whilst 75% of the population of the former Soviet Union live in the south and west of the country, only 16% of the ex-nation's river flow crosses these regions (Micklin, 1987, 1988).

A conspicuous consequence of this imbalance between supply and demand is the Aral Sea Crisis, where between 1960 and 1987, the diversion of inlowing river water for irrigation led to a drop in sea level of $13m$ (Micklin, 1987, 1988). As a result, the sea, which had been the world's fourth largest lake by area, suffered a 40% reduction in surface area (Micklin, 1988). A further direct consequence of the declining river inflow was a tenfold increase in the salinity of some regions of the Aral Sea (Micklin, 2007). These changes had wide-ranging regional impacts including the collapse of commercial fisheries; a loss of endemic vegetation communities, which were replaced by dry and salty condition loving halophyte and xerophyte plants; changes in regional climate; and the formation of vegitation sparese salt pans on the dried seabed, which lead to aeolian plumes of dust, salt and sand which adversely impacted human health (Micklin, 1988, 2007).

A geoengineering solution to the falling water levels in the Aral and Caspian Seas had been proposed in various forms, with the first proposal in Tsarist times. The most extreme of these involved a $315km^3yr^{-1}$ river diversion plan (Micklin, 1987). In 1984, work began on such a plan, known as the "Sibaral", or Northern River reversal. The plan was to divert four of the largest Russian rivers flowing into the Arctic Ocean; the Northern Dvina, Pechora, Ob' and Yenisey rivers, south to the Aral and Caspian Seas (figure 1 b) (Cattle, 1985; Micklin, 1988). Whilst this project was halted in 1986 by Mikhail Gorbachev amid concerns over the potential environmental and economic costs (Micklin, 1988, 2007), there remains a high-level interest in the revival of the project (Micklin, 2007, 2011; Pearce, 2004). Meanwhile, increasing pressures on global water resources due to the growing human population and climate change, make it increasingly likely water management solutions of this scale will become necessary.

Freshwater in the Arctic Ocean plays a key role in determining the circulation, and in particular, the fate of heat associated with warmer, salty, Atlantic Water (AW), which enters the Arctic Ocean at depth (Carmack, 2007; Lenn et al., 2009; Rudels et al., 2015). The Yenisey and Ob' are amongst the largest rivers on the world (Dai et al., 2009), each with a watershed area and annual discharge comparable to the largest US River, the Mississippi (Holmes et al., 2012). Indeed they dwarf many of the large temperate Eurasian rivers such as the Rhine (Dai & Trenberth, 2002), meaning these four rivers play an important role in determining the circulation and fate of Atlantic Water heat in the Arctic Ocean.

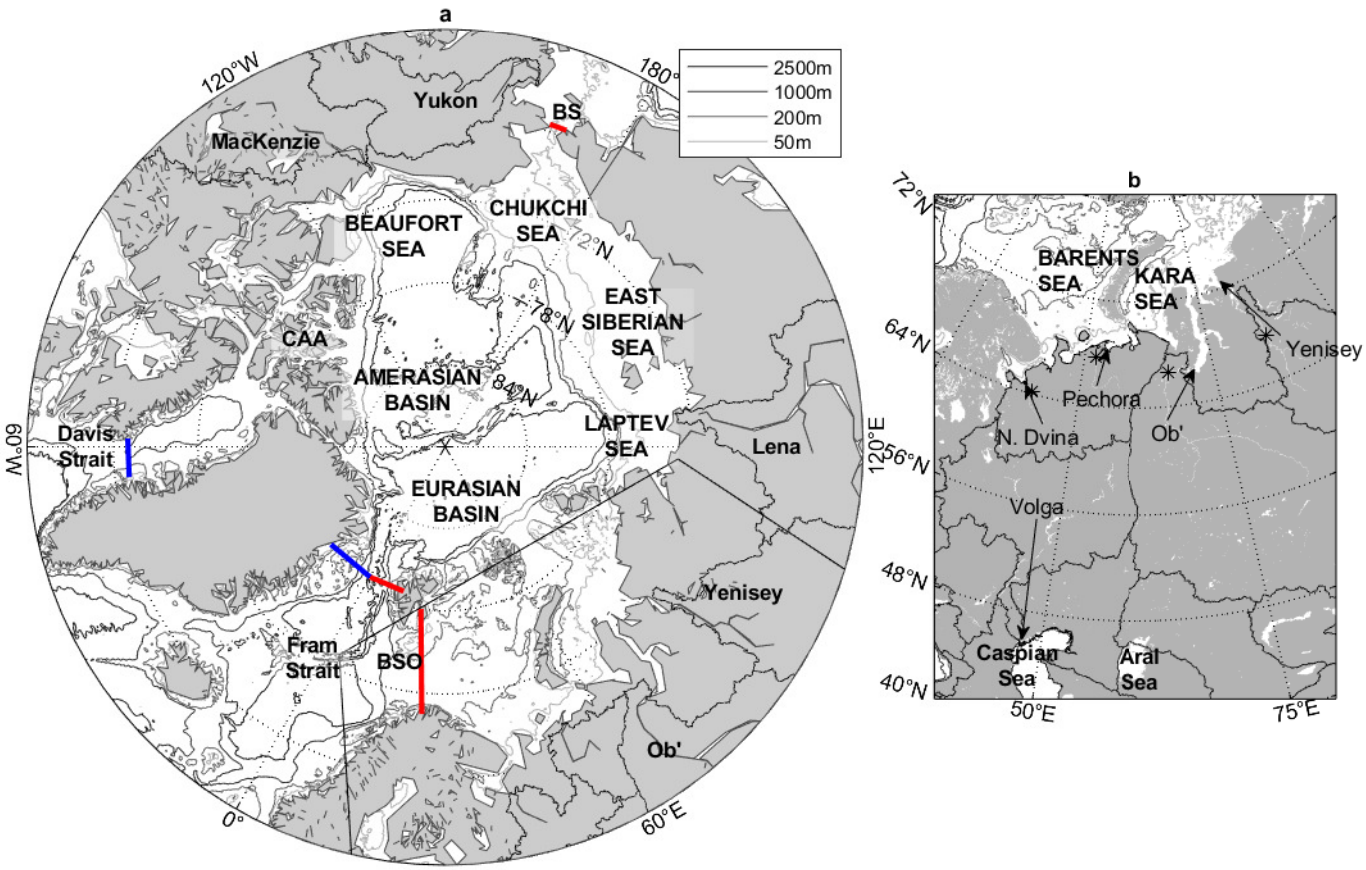

Figure 1. Map of a) the Arctic Ocean, showing inflow (red) and outflow (blue) gateways, the largest rivers, and major features of the Arctic Ocean. b) showing enlarged Siberian region of interest to this study, with main drainage basins outlined, the Aral and Caspian Seas shown, and the direction and location of river mouths (arrow heads) and furthest downstream stations (*) for the Ob' (Salehard Station), Yenisey (Igarka Station), Pechora (Oksino Station) and S. Dvina (Ust'-Pinega Station) rivers.

The Arctic is one of the fastest warming regions on the planet (Dai et al., 2019; Serreze & Barry, 2011), with perhaps the most conspicuous consequence a large decline in seasonal sea ice cover over the Arctic Ocean in recent years (Cavalieri & Parkinson, 2012; Gao et al., 2015; Onarheim et al., 2018; Stroeve & Notz, 2018; Wang et al., 2019; Zygmuntowska et al., 2014), with a 45% decline in September Sea Ice extent from the 1970s to 2016 (Onarheim et al., 2018). Far field impacts linked to sea ice decline include potential changes in northern hemisphere atmospheric circulation patterns (Budikova, 2009; Cohen et al., 2014; Screen et al., 2018; Tang et al., 2013; Vihma, 2014; Zhang et

al., 2018), a weakening of the Atlantic Meridional Overturning Circulation, which transports heat and moisture to the high latitudes (Sévellec et al., 2017) and a change in the regional energy budget due to the albedo effect (Serreze & Barry, 2011). These changes have been linked to recent prolonged cold conditions in northern Europe and Siberia (Chen et al., 2018; Francis et al., 2018; Petoukhov & Semenov, 2010), and smog in the East China Plains (Zou et al., 2017). Many of these changes are linked to the changes in albedo resulting from the melting of sea ice. When highly reflective sea ice melts it exposes the relatively absorbent underlying water, resulting in a reduction in the albedo (the proportion of incoming solar radiation that is reflected at the surface), and in consequence, more solar radiation is absorbed, leading to a warming of the surface waters by up to 4-5°C in newly ice-free regions (Cohen et al., 2014; Serreze & Francis, 2006). As the daylength reduces in the autumn, the excess oceanic heat warms the lower atmosphere, slowing sea ice formation, consequently impacting the regional energy budget (this is a process of Arctic Amplification).

Assessments of the impact of this diversion project on the Arctic Ocean have been carried out in the past (e.g. Cattle, 1985). However, they were not able to take advantage of recent insights into the potential role of freshwater in regulating the oceanic heating which drives sea ice decline in the Arctic Ocean (e.g. Barton et al., 2018; Polyakov et al., 2017). The aim of this paper is to investigate the potential impact of the redirection of the Siberian Rivers on the aerial extent of sea ice cover in the Eurasian basin of the Arctic Ocean, through the weakening upper ocean stratification. To achieve this, we will first review the water column structure in the Arctic Ocean, and in particular, the isolation of the heat associated with the largest ocean heat source to the Arctic Ocean, intruding intermediate depth Atlantic Water from the sea surface and sea ice. We will then assess the consequences of the redirection of the Siberian Rivers on the upper ocean water column structure in the Eurasian Basin and use a simple mixing model to assess the impact of the changes to water column structure and by implication, on the fate of heat associated with the intruding intermediate depth Atlantic Water.

2 The role of Freshwater in the Arctic Ocean

The Eurasian rivers flowing into the Arctic Ocean account for 11% of global river discharge and yet drain into a basin containing only 1% of the global ocean volume (Carmack et al., 2016). Furthermore, the Eurasian continental shelf seas, which receive a large pro-

portion of this river inflow account for a significant area of this proportion of the Arctic Ocean (figure 1 a). These seas receive the freshwater inflow from some of the Arctic's biggest rivers, namely the Northern Dvina, Pechora, Ob', Yenisey, Lena, Khatanga, and Kolyma Rivers, for which gauged flow records stretch back more than 80 years in some cases (Dai & Trenberth, 2002). These rivers are all derived from drainage systems originating in the mid latitudes (figure 1 b) and consequently force a mid-latitude signal on the Arctic Ocean (Carmack et al., 2016).

The Arctic Ocean differs from many oceans globally in several respects. Whilst ocean temperature dominates the density structure across many of the world's oceans, the Arctic Ocean is a beta ocean, indicating that the density stratification is dominated by salinity differences. This is a consequence of the low temperatures, which create small thermal expansion coefficients relative to the coefficient of haline contraction (Carmack, 2007). The surface waters tend to be fresher and cold, with the temperature increasing with depth across the cold halocline layer (CHL), which sits above the temperature maximum associated with an intruding Atlantic Water layer.

The Arctic Ocean has limited linkage to the rest of the world's oceans (figure 1 a). The Fram Strait, which lies between Greenland and Svalbard, represents the main gateway, linking the Arctic Ocean to the North Atlantic. Relatively warm Atlantic Water enters the Arctic Ocean through this gateway and the Barents Sea Opening (BSO) and sinks to intermediate depths as it enters the Arctic Ocean. Although warmer than the resident Arctic Ocean water, it is also saltier and therefore denser (Rudels et al., 2015). The intruding Atlantic Water supports a net northward heat transport of 21 ± 5 TW into the Arctic Ocean (Schauer et al., 2004). A number of studies have considered the impact of heat transfer from the Atlantic Water to the Surface Mixed Layer (SML) on sea ice thickness (e.g. Aagaard et al., 1981; Carmack et al., 2015; Rudels et al., 2015) and have shown there to be sufficient heat contained within the AW layer to melt the sea ice completely if this heat were to flux to the surface (Carmack et al., 2016; Nummelin et al., 2015; Polyakov et al., 2017; Turner, 2010).

Vertical mixing in the Arctic is weak when compared to much of the world's oceans. Vertical heat fluxes from intermediate depths in the central Eurasian Basin have been estimated to be around $1 W m^{-2}$ (Polyakov et al., 2013, 2019). Due in part to the low levels of turbulent mixing, vertical heat fluxes from the intruding Atlantic Water are con-

strained by the formation of double-diffusive staircases. These structures form across the halocline in much of the Arctic Ocean (Shibley et al., 2017) including the Eurasian Basin (Lenn et al., 2009), and are a consequence of differing rates of molecular diffusion of heat and salt. Turbulent mixing is suppressed by the strong haline stratification, a consequence of the high upper ocean freshwater content. Recent measurements have revealed a weakening of the halocline stratification with a coincident increased sea ice melt in the Eurasian Basin (Polyakov et al., 2017) highlighting the sensitivity of the fate of this region's sea ice to changes in halocline stratification. Steele and Boyd (1998) also identified weakening (and in some regions complete retreat) of the Cold Halocline Layer in the Eurasian Basin during the early 1990s. The weakening was attributed to changes in atmospheric circulation that directly led to long term changes in the delivery of fresh Siberian shelf sea waters to the Eurasian Basin (Boyd et al., 2002; Steele & Boyd, 1998). This indicates a sensitivity of the Cold Halocline Layer in the Eurasian Basin to changes in freshwater supply from the shelf to the Eurasian Basin, itself dependent on input of freshwater from Siberian rivers (Rudels et al., 1996; Steele & Boyd, 1998).

Whilst the intruding Atlantic Water lies at depths of 200m or more, and is isolated from turbulent mixing linked to storms across much of the Arctic Ocean (Davis et al., 2016; Lincoln et al., 2016), it resides closer to the surface in the Eurasian Basin (e.g. Lenn et al., 2009; Polyakov et al., 2018). As a result, the water column in the Eurasian Basin is more susceptible to turbulence stirring Atlantic Water heat to the surface (Davis et al., 2016).

3 Methods

3.1 Arctic River Flow

Monthly river discharge data from the four rivers initially included in the diversion project (the Yenisey, Ob', Pechora and Northern Dvina rivers) was retrieved from the Arctic Rapid Integrated Monitoring System (ArcticRIMS- http://rims.unh.edu/data) for the period 1900-1999 whilst data was available. This data was sourced from the furthest downstream station on the network for each river (Dai & Trenberth, 2002) (figure 1 and converted into km^3 $month^{-1}$. The mean and standard deviation of climatic monthly discharge for each river each month was calculated and plotted in figure 2. The average and standard deviation of annual discharge for each river was also calculated.

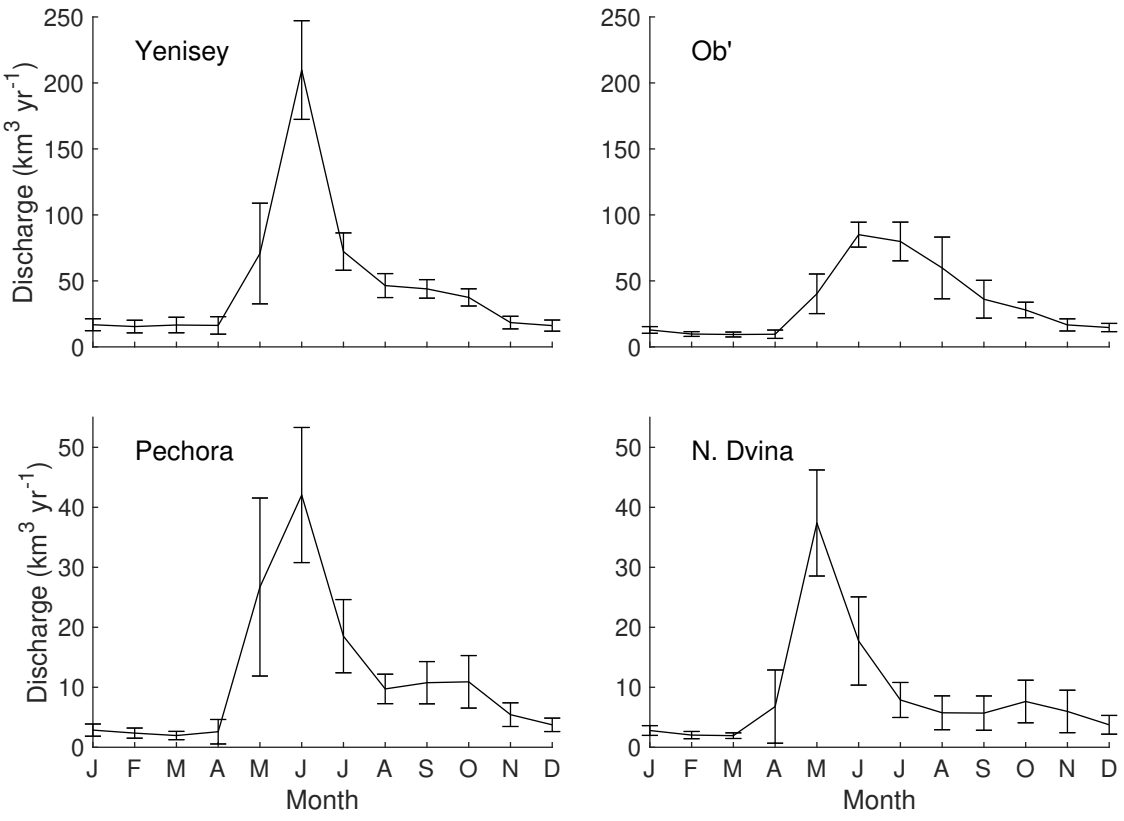

Figure 2. Annual pattern of discharge from the four rivers from the Arctic RIMS database, using available data collected from 1900 to 1999. Error bars show the standard deviation of monthly discharge.

The impact of turning off the four rivers planned for diversion was calculated using the average annual discharge data alongside the Arctic freshwater budget produced by Haine et al. (2015). This was done by calculating the contribution of these four study rivers to the total river flow into the Arctic Ocean giving the proportion of total Arctic river flow from the study rivers (P_{SR}). Pemberton et al. (2014) identified that 81% ($19.2 \times 10^3 km^3$) of the total freshwater input to the Eurasian Basin ($23.5 \times 10^3 km^3$) was from Eurasian Rivers (this 81% here defined as P_{ER}). Thus the percentage of total freshwater that would be removed from the Eurasian Basin by turning off this river supply would be $R_f = P_{ER} \times P_{SR} = 25.9\%$.

3.2 Impact on Water Column Structure

Water column structure is derived from the MIMOC v2.2 climatology (Schmidtko et al., 2013), averaged across the Eurasian Basin defined as $0 - 120$°E and $85 - 90$°N (as in Davis et al., 2016). This climatology provides absolute salinity and conservative temperature at 0.5°resolution at 81 standard pressure levels from $0-1950 dbar$. In high latitudes, where Ice-Tethered Profiler (ITP) data is not abundant, the climatology may represent a historic state of the ocean owing to its use of historic data. The Gibbs Sea-Water Oceanographic Toolbox (McDougall & Barker, 2011) was used to calculate density and the N^2 buoyancy frequency. This N^2 buoyancy frequency is a measure of stability (the competition between buoyancy acting to stratify, and turbulent mixing acting to mix (Dzwonkowski et al., 2018)) in a water column. Specifically, it gives the frequency at which a vertically displaced water parcel oscillates due to the inequality of buoyancy with the surrounding water. This value increases as stability (and therefore density gradient) increases.

To simulate the impact of the removal of freshwater from the four Siberian rivers, the water column salinity is recalculated (figure 3) using:

$$S_{new}(z) = S(z) + R_f(S_0 - S(z)) \tag{1}$$

Where $S_{new}(z)$ is the altered salinity at depth z, $S(z)$ is the unadjusted salinity at depth z, R_f is the freshwater reduction factor of 0.259, and S_0 is the deep-water salinity value, taken at the depth of the temperature maximum for that profile (as below this depth, it was assumed that freshwater changes would not have an effect).

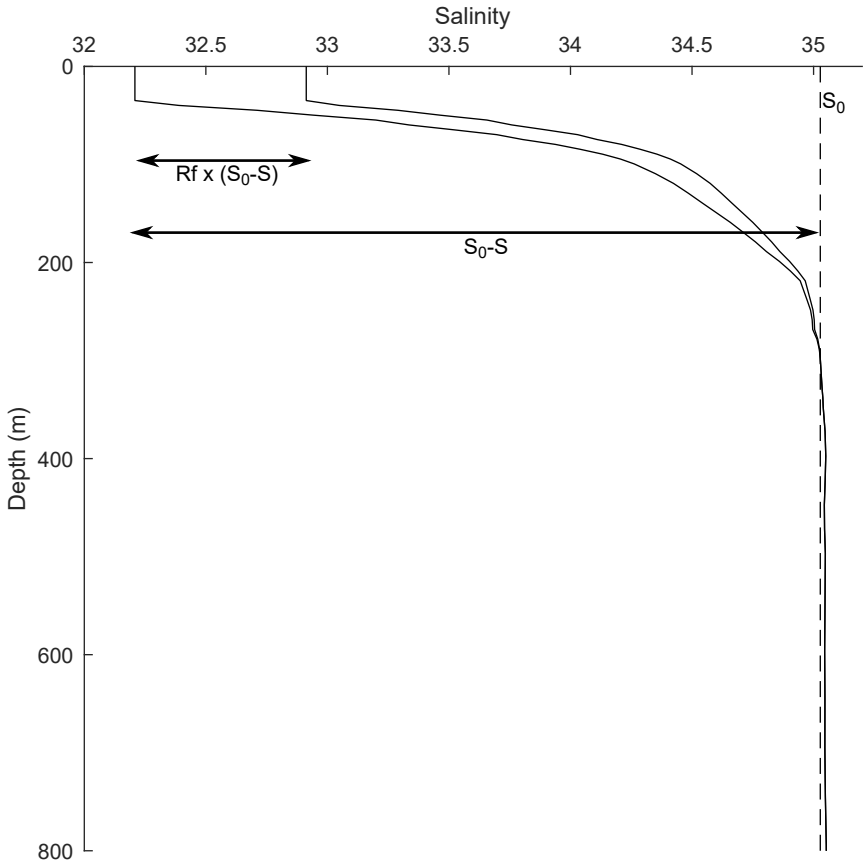

Figure 3. Schematic showing modelled changes in salinity under Reduction factor (R_f).

This was calculated for two scenarios dependent on the depth to which salinity adjustments took place: Surface Mixed Layer (SML) mixed scenario; and Cold Halocline Layer (CHL) mixed scenario.

3.2.1 Surface Mixed Layer (SML) Mixed Scenario

A SML mixed scenario was run, where changes to freshwater were constrained to the surface layer. This layer was defined as the water above the depth of the maximum N^2 buoyancy frequency, indicating the greatest density gradient, which is known to occur at the pycnocline.

The increase in surface salinity (and therefore density) associated with river diversion resulted in a hydrostatic instability (where more dense water lay above less dense water) forming in this scenario. This was removed by deepening the SML through entraining of water from deeper layers until the instability was resolved. Temperatures and

salinities of the new, deeper mixed layer were recalculated, representing the combination of the properties of the old SML and the properties of the entrained underlying water. Sensitivity runs at a range of R_f (from 0.5% to 25.9%) were run for this scenario to determine the surface salinity change that would be required to form an instability, and therefore entrainment of warmer, denser water. The effect of the entrainment of warmer water into the surface mixed layer in the destabilised surface mixed layer scenario on sea ice was assessed using eq. 2 and 3 (Davis et al., 2016). These equations calculate the change in heat content in the mixed layer, and the resulting impact on sea ice thickness through melting.

$$\Delta H_c = \rho_0 C_p \left\{ \int_{z=-h}^{z=0} \big[\theta(t) - \theta_f(t)\big] dz - \int_{z=-h}^{z=0} \big[\theta(0) - \theta_f(0)\big] dz \right\} \tag{2}$$

$$\Delta h_I = \frac{\Delta H_c}{\rho_I L_I} \tag{3}$$

Where H_c is the heat content of the mixed layer. ρ_0 is oceanic seawater density ($1027 kgm^{-3}$), and C_p the ocean specific heat capacity ($3895 Jkg^{-1}K^{-1}$), z the depth below the surface, θ is potential temperature, and θ_f the in situ freezing temperature (varying upon salinity). h_I is the thickness of sea ice, where ρ_I is the ice density ($900 kgm^{-3}$), and L_I the latent heat of fusion of sea ice ($3 \times 10^5 Jkg^{-1}$). The bracketed t refers to the scenario, compared to (0) referring to the present-day scenario.

3.2.2 Cold Halocline Layer (CHL) Mixed Scenario

A CHL mixed scenario was run where salinity was reduced for depths less than the base of the Cold Halocline Layer, defined as the depth of the temperature maximum. In this scenario, no instability was present, and so the above entrainment scheme was not applied.

3.3 Mixing Model

In order to assess the sensitivity of the Eurasian Basin water column to changes in the stratification resulting from reduced freshwater input, a Potential Energy Anomaly (Φ) (eq. 4) is used to quantify the strength of stratification, and compare it to the available energy to drive turbulent mixing (Simpson, 1981). Φ represents the amount of en-

ergy required to completely mix the water column down to the temperature maximum, and therefore flux Atlantic Water (and its associated heat) to the surface.

$$\Phi = \frac{1}{h}\int_{-h}^{0} \big(\hat{\rho} - \rho(z)\big) g z dz \tag{4}$$

$$\hat{\rho} = \frac{1}{h}\int_{-h}^{0} \rho dz \tag{5}$$

Where h is the depth of the base of the Cold Halocline Layer, g is the gravitational constant ($9.81 ms^{-2}$ and $\rho(z)$ is the density at depth z.

Heating and stirring from wind stress was assessed as the change of Φ where $\Phi(t)$:

$$\Phi(t) = \Phi_0 + \left(\frac{\alpha g}{2C_p}\int_0^t Q_i dt - \frac{e_s k_s \rho_a}{h}\int_0^t W^3 dt \right) \tag{6}$$

Where $\Phi(0)$=Φ_0, α is the thermal volume expansion coefficient, C_p is specific heat of seawater, e_s is the efficiency of wind mixing, assumed to be 0.023 (Simpson & Sharples, 2012), k_s is the modified surface drag coefficient, ρ_a is the density of air (1.3 kg m^{-3}), and h is depth as given before. W^3 is wind speed cubed, and Q_i is the rate of heating at the surface, calculated as the sum of the heating terms (net shortwave Radiation, downward longwave radiation, upward longwave radiation, latent and sensible heat), which were determined from the CORE.2 Global Air-Sea Flux Dataset (Yeager & Large, 2008).

10m above surface Wind data for the Eurasian Basin at six-hourly intervals during the time during which the Great Arctic Cyclone of 2012 took place (1st-20th August 2012) were retrieved from NCEP/NCAR Reanalysis 1 for 85°N, 60°E. This period was chosen for ease of comparison to the in situ measurements taken by Lincoln et al. (2016). The sensitivity of the water column to wind mixing, and the relative impacts of these changes of freshwater supply were assessed using various wind forcings under the model of eq. 6. Over a period of 20 days in August (when water column structure is weakest), the change in Φ for actual, half and double NCEP speed scenarios were carried out. Alongside this, 6 sensitivity runs with constant wind speed were carried out, at 0.5, 1, 5, 10, 15 and $20 ms^{-1}$. These represented very calm conditions (0.5, $1.0 ms^{-1}$), the maximum NCEP wind speed during this period ($10 ms^{-1}$), as well as half ($5 ms^{-1}$), double ($20 ms^{-1}$) and 1.5 times ($15 ms^{-1}$) this wind speed.

4 Results

4.1 Arctic River Flow

Mean monthly river discharge (figure 2) had strong seasonal variation in flow, with 90% of annual delivery by the rivers to the Arctic Ocean occurring from spring onwards, representing a mid-high latitude spring onset. This is in contrast to the sea ice melt season in the Arctic Ocean (which is also a major source of freshwater in the Arctic), which begins around June. The Yenisey river discharged $580.1 \pm 42.5 km^3 yr^{-1}$ to the Arctic, and is the largest contributor of freshwater of the four rivers impacted by the plans for diversion. The Ob' river contributes $401.8 \pm 59.3 km^3 yr^{-}1$ and the remaining two rivers, the Pechora and Northern Dvina rivers had annual flows of $125.3 \pm 27.1 km^3 yr^{-1}$ and $105.2 \pm 19.3 km^3 yr^{-1}$ respectively. Based on Haine et al. (2015) calculations of total river flow to the Arctic Ocean, between them, these four rivers account for 31% of the total river inflow to the Arctic Ocean.

4.2 Impact on Water Column Structure

Removal of freshwater from the water column acted to increase surface salinity, reducing the salinity gradient (and therefore density gradient) between the surface and bottom waters (figure 4).

4.2.1 Surface Mixed Layer (SML) Mixed Scenario

Instabilities formed in the top of the water column during the SML mixed scenario, as the density in this layer, once salinity was increased, became higher than the immediately underlying waters where salinity had not been altered. Entrainment due to convective fluxes from the warmer, less dense CHL water up into the SML warmed this surface layer to the extent that a 6.01 cm per year net sea ice melt was expected to occur, Although this figure is small in comparison to the half meter sea ice loss in six months predicted by Davis et al. (2016), our estimated value forms only a lower bound for sea ice loss, owing to not considering any additional heat flux resulting from weakened stratification.

Sensitivity runs to test the threshold at which these instabilities would form found that only 0.76% change in surface freshwater content was required to form an instabil-

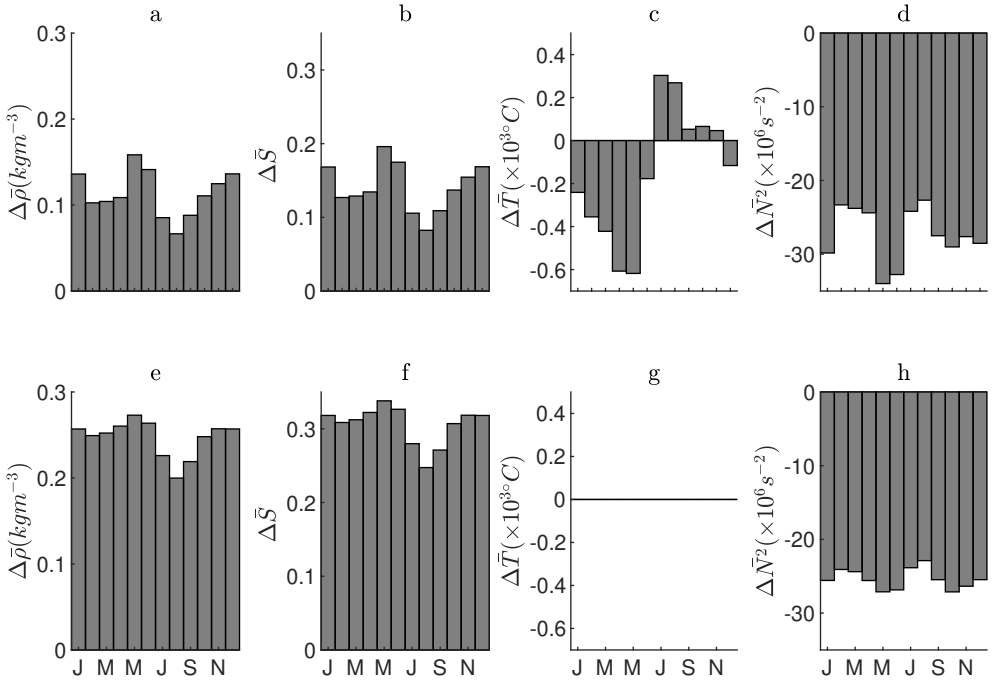

Figure 4. Changes to depth averaged (to 250m depth) properties of water column profiles across the climatic year associated with removing river flow compared to the present-day scenario. Showing changes for the SML mixed scenario (a-d), where the freshwater was removed from the Surface Mixed Layer (SML) only, and from the SML and Cold Halocline Layer (CHL mixed scenario) (e-h).

ity (and therefore entrainment into the upper layer) for some months, whilst for a year-round instability to form, 11.9% change in surface freshwater was required.

The entrainment of deeper waters into the SML in the SML mixed scenario led to an increase in the temperature and depth of this layer (figure 4 c), resulting in a reduction in the extent to which the density was increased in this scenario (figure 4 a) compared to the CHL mixed scenario. Deepening of the base of the SML in this scenario also led to the observed decrease in N^2 near to the surface, and increase at deeper depths (figure 4 d). There was also an associated overall weakening of the pycnocline (figure 4 d) compared to the present-day scenario.

4.2.2 Cold Halocline Layer (CHL) Mixed Scenario

The temperature profiles in the CHL mixed scenario is the same as in the present day (figure 4 g), whilst removal of freshwater acted to increase salinity and density down

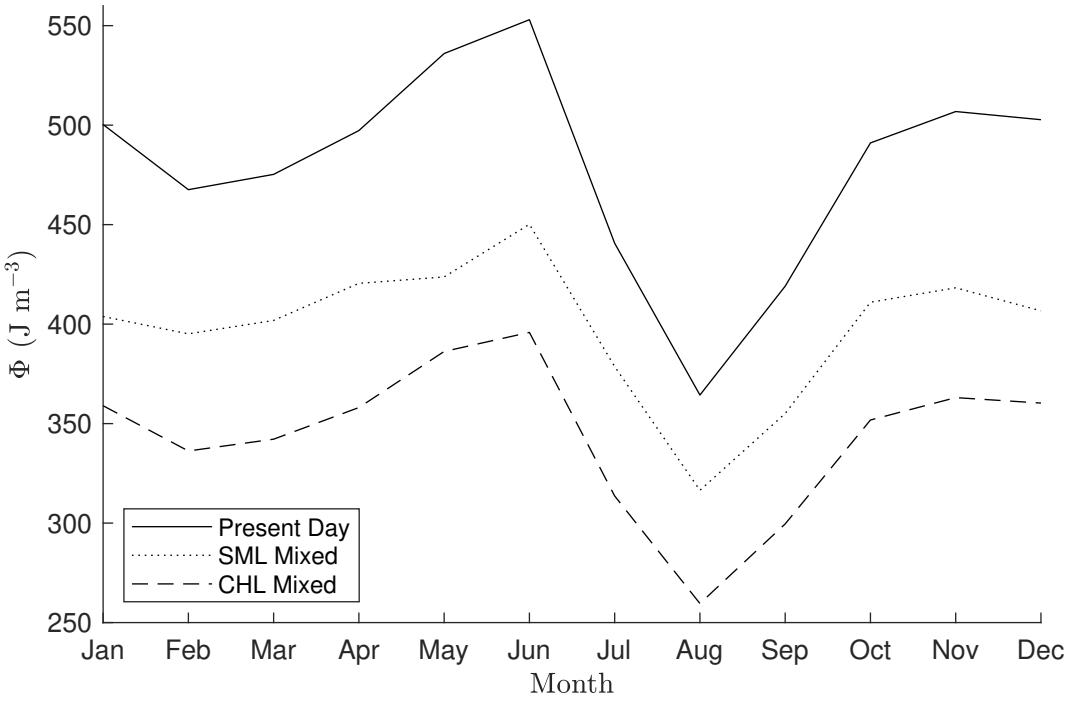

Figure 5. Annual variation in Potential Energy Anomaly for Eurasian Basin under present-day climatology, and under the SML mixed and CHL mixed scenarios.

to 250-350m (figure 4 f). This considerably reduced the density gradient from the surface to Atlantic Water. Peak N^2 buoyancy frequency, whilst remaining at the same depth, decreased, indicating that this reduction in salinity resulted in a less stable water column (figure 4 h).

4.3 Mixing Model

In the present-day scenario, the potential energy anomaly (Φ) of the Eurasian Basin average profile was an average of $480 Jm^{-3}$, with a seasonal range of $188 Jm^{-3}$ (figure 5). Stratification peaks during June and is weakest in August. Changes in Φ were most pronounced in the CHL mixed scenario, reducing by $104.7 - 157.1 Jm^{-3}$ compared to the present-day scenario, and with an annual average Φ of $344 Jm^{-3}$. This falls outside of the present-day annual range. In the SML mixed scenario, effects are less strong, but still represent reductions of $49.3{-}122.2 Jm^{-3}$, with an average of $398 Jm^{-3}$, a value only presently observed in August. Additionally, the results presented here do not account for spatial and interannual variability, each of which may make particular regions or time periods more susceptible to mixing.

For the NCEP conditions, the change in Φ was $-0.38 Jm^{-3}$, a very small amount in comparison to the changes resulting from river diversion. Sensitivity runs on this data at $0.5\times$ and $2\times$ the observed wind speeds resulted in $\Delta\Phi$ of $0.044 Jm^{-3}$ and $-3.78 Jm^{-3}$ respectively. At 0.5 and $1.0 ms^{-1}$ constant wind speed, the solar heating of the water column overcomes the impact of wind mixing, leading to an increase of 0.104 and $0.102 Jm^{-3}$ respectively. At constant wind speeds of $5 ms^{-1}$, $\Delta\Phi$ is $-0.184 Jm^{-3}$. Beyond $10 ms^{-1}$, $\Delta\Phi$ becomes more important, from $-2.21 Jm^{-3}$ at $10 ms^{-1}$ to $-7.69 Jm^{-3}$ at $15 ms^{-1}$, and $-18.4 Jm^{-3}$ at $20 ms^{-1}$. The observed reduction in stratification strength for the CHL mixed scenario is equivalent to winds of $36 ms^{-1}$ blowing for 20 days. The $1\times$NCEP reanalysis wind results are likely to be an underestimate, as the six-hourly averages will not represent the wind's true variance (Gille, 2005), leading to a significant underestimation of mixing which relies on W^3. Yet, even the highest wind speeds have impacts over an order of magnitude less than the change of river discharge impact, illustrating the extent of these changes.

5 Summary and Conclusions

Here, the far-reaching effects of turning off the supply of freshwater from four Siberian rivers considered for diversion in the Sibaral project have been considered quantitatively for the first time. With the Yenisey, Ob', Pechora and Northern Dvina rivers contributing a combined 31.7% of the total runoff from Eurasian rivers, removing this would have effects on the water column structure in the Arctic, where the density structure is dependent on salinity. Crucially in the Arctic, water column structure and stability have a major role in determining the heat budget, and the flux of heat from the warm, salty Atlantic Water layer, and the sea ice at the surface.

This paper consisted of two scenarios for if the rivers had been diverted, where changes were constrained to only the Surface Mixed Layer, or across the Cold Halocline Layer. The CHL scenario presents the most severe consequences in terms of reductions in stability, where across almost the entire year, the new stratification is weaker than the weakest stratification observed in the climatological year. It is also the case that evidence of past changes in the Arctic structure, and particle tracking models suggest that this scenario would be most likely. Boyd et al. (2002) found that the breakdown of the CHL in the Eurasian Basin during the 1990s was due to changes in freshwater delivery from Siberian Rivers, showing that this would be the most likely outcome of the project. This also pro-

vides evidence that CHL decline, and complete disappearance could be a possible outcome of river diversion. Steele and Boyd (1998) found that this breakdown of the CHL resulted in a 30-40% increase in upward heat flux to the Arctic Sea ice base compared to the average. Weakening of the CHL has also been reported by (Polyakov et al., 2017) which showed an increase of upward heat fluxes from the CHL by a factor of $2-4$ as a result of these changes, explaining a $54cm$ reduction in sea ice.

Meanwhile, the SML mixed scenario presents another scenario with considerably reduced stratification, but with immediate ice melt identified from the resulting entrainment of warmer water. Whilst this melt is small in comparison to those expected from full erosion of the Cold Halocline Layer and entrainment of this heat (Davis et al., 2016), this calculation would be additional to any increased heat flux, not calculated here, as a result of the reduced stratification.

The Arctic region is currently undergoing changes at a rapid pace, warming faster than any other region on the globe (Serreze & Barry, 2011), and as a result, has been the focus of a lot of recent research. A large body of this research considers the global and regional impacts on weather and climate of sea ice loss, and this can be applied to this study. Uncertainty over the nature and extent of these links (Blackport et al., 2019; Screen et al., 2018; Francis, 2017) only emphasises the complexity and far reaching effects these geoengineering projects may have. Sea ice decline resulting from the project and the resultant changes in water column structure can be expected to have the most far-field impacts due to this climatic link. With the absence of sea ice, surface waters lose a barrier for exchange of heat and momentum with the atmosphere. This leads to heating of both the surface waters and the lower atmosphere, and so warmer, moister air masses over the Arctic spread to nearby continents (Cohen et al., 2014; Vihma, 2014).

At a time of changing climate and increasing pressures on existing water resources, we thought it timely to revisit a major geoengineering solution proposal and investigate the potential far-field impacts. We found convincing evidence for considerable changes to Arctic Ocean stratification occurring due to the proposed turning off of four Siberian rivers, resulting in far field impacts on weather and climate due to loss of sea ice.

Acknowledgments

S. Hartharn-Evans was supported by a Natural Environment Research Council (NERC) studentship through the ONE Planet Doctoral Training Partnership. We would like to thank Yueng Djern-Lenn (Bangor) for both advice on data products during early stages of the project, and for helpful feedback on the manuscript. All data used are freely available in an accessible format with associated metadata, and can be accessed as follows: river data can be downloaded from the Arctic Rapid Integrated Monitoring System (http://rims.unh.edu/data.sht the CORE.2 global air-sea flux dataset can be downloaded from https://rda.ucar.edu/datasets/ds260.2/, the NCEP/NCAR Wind Data from https://psl.noaa.gov/data/gridded/data.ncep.reanalysis.html and the MIMOC v2.2 ocean climatology can be downloaded from https://www.pmel.noaa.gov/mimoc/

References

Aagaard, K., Coachman, L. K., & Carmack, E. C. (1981, 6). On the halocline of the Arctic Ocean. *Deep Sea Research Part A, Oceanographic Research Papers*, *28*(6), 529–545. Retrieved from `https://www.sciencedirect.com/science/article/pii/0198014981901151` doi: 10.1016/0198-0149(81)90115-1

Barton, B. I., Lenn, Y.-D., & Lique, C. (2018, 8). Observed Atlantification of the Barents Sea Causes the Polar Front to Limit the Expansion of Winter Sea Ice. *Journal of Physical Oceanography*, *48*(8), 1849–1866. Retrieved from `http://journals.ametsoc.org/doi/10.1175/JPO-D-18-0003.1` doi: 10.1175/jpo-d-18-0003.1

Blackport, R., Screen, J. A., van der Wiel, K., & Bintanja, R. (2019, 9). Minimal influence of reduced Arctic sea ice on coincident cold winters in mid-latitudes. *Nature Climate Change*, *9*(9), 697–704. doi: 10.1038/s41558-019-0551-4

Boyd, T. J., Steele, M., Muench, R. D., & Gunn, J. T. (2002, 7). Partial recovery of the Arctic Ocean halocline. *Geophysical Research Letters*, *29*(14), 94–97. Retrieved from `http://doi.wiley.com/10.1029/2001GL014047` doi: 10.1029/2001GL014047

Budikova, D. (2009, 8). Role of Arctic sea ice in global atmospheric circulation: A review. *Global and Planetary Change*, *68*(3), 149–163. Retrieved from `https://www.sciencedirect.com/science/article/pii/S0921818109000654` doi: 10.1016/J.GLOPLACHA.2009.04.001

Carmack, E. C. (2007, 11). The alpha/beta ocean distinction: A perspective on

freshwater fluxes, convection, nutrients and productivity in high-latitude seas. *Deep-Sea Research Part II: Topical Studies in Oceanography*, *54*(23-26), 2578–2598. Retrieved from https://www.sciencedirect.com/science/article/pii/S0967064507002019 doi: 10.1016/j.dsr2.2007.08.018

Carmack, E. C., Polyakov, I. V., Padman, L., Fer, I., Hunke, E., Hutchings, J., ... Winsor, P. (2015, 12). Toward quantifying the increasing role of oceanic heat in sea ice loss in the new arctic. *Bulletin of the American Meteorological Society*, *96*(12), 2079–2105. Retrieved from http://journals.ametsoc.org/doi/10.1175/BAMS-D-13-00177.1 doi: 10.1175/BAMS-D-13-00177.1

Carmack, E. C., Yamamoto-Kawai, M., Haine, T. W. N., Bacon, S., Bluhm, B. A., Lique, C., ... Williams, W. J. (2016, 3). Freshwater and its role in the Arctic Marine System: Sources, disposition, storage, export, and physical and biogeochemical consequences in the Arctic and global oceans. *Journal of Geophysical Research: Biogeosciences*, *121*(3), 675–717. Retrieved from http://doi.wiley.com/10.1002/2015JG003140 doi: 10.1002/2015JG003140

Cattle, H. (1985, 5). Diverting soviet rivers: Some possible repercussions for the arctic ocean. *Polar Record*, *22*(140), 485–498. Retrieved from http://www.journals.cambridge.org/abstract_S0032247400005933 doi: 10.1017/S0032247400005933

Cavalieri, D. J., & Parkinson, C. L. (2012). *Arctic sea ice variability and trends, 1979-2010* (Vol. 6) (No. 4). Retrieved from www.the-cryosphere.net/6/881/2012/ doi: 10.5194/tc-6-881-2012

Chen, L., Francis, J., & Hanna, E. (2018, 11). The "Warm-Arctic/Cold-continents" pattern during 1901–2010. *International Journal of Climatology*, *38*(14), 5245–5254. Retrieved from http://doi.wiley.com/10.1002/joc.5725 doi: 10.1002/joc.5725

Cohen, J., Screen, J. A., Furtado, J. C., Barlow, M., Whittleston, D., Coumou, D., ... Jones, J. (2014, 9). Recent Arctic amplification and extreme mid-latitude weather. *Nature Geoscience*, *7*(9), 627–637. Retrieved from http://www.nature.com/articles/ngeo2234 doi: 10.1038/ngeo2234

Dai, A., Luo, D., Song, M., & Liu, J. (2019, 12). Arctic amplification is caused by sea-ice loss under increasing CO 2. *Nature Communications*, *10*(1), 1–13. doi: 10.1038/s41467-018-07954-9

Dai, A., Qian, T., Trenberth, K. E., & Milliman, J. D. (2009, 5). Changes in continental freshwater discharge from 1948 to 2004. *Journal of Climate*, *22*(10), 2773–2792. Retrieved from http://journals.ametsoc.org/doi/abs/10.1175/2008JCLI2592.1 doi: 10.1175/2008JCLI2592.1

Dai, A., & Trenberth, K. E. (2002, 12). Estimates of Freshwater Discharge from Continents: Latitudinal and Seasonal Variations. *Journal of Hydrometeorology*, *3*(6), 660–687. Retrieved from http://journals.ametsoc.org/doi/abs/10.1175/1525-7541%282002%29003%3C0660%3AEOFDFC%3E2.0.CO%3B2 doi: 10.1175/1525-7541(2002)003⟨0660:EOFDFC⟩2.0.CO;2

Davis, P. E. D., Lique, C., Johnson, H. L., & Guthrie, J. D. (2016, 5). Competing Effects of Elevated Vertical Mixing and Increased Freshwater Input on the Stratification and Sea Ice Cover in a Changing Arctic Ocean. *Journal of Physical Oceanography*, *46*(5), 1531–1553. Retrieved from http://journals.ametsoc.org/doi/10.1175/JPO-D-15-0174.1 doi: 10.1175/JPO-D-15-0174.1

Dzwonkowski, B., Fournier, S., Park, K., Dykstra, S. L., & Reager, J. T. (2018, 8). Water Column Stability and the Role of Velocity Shear on a Seasonally Stratified Shelf, Mississippi Bight, Northern Gulf of Mexico. *Journal of Geophysical Research: Oceans*, *123*(8), 5777–5796. Retrieved from https://onlinelibrary.wiley.com/doi/abs/10.1029/2017JC013624 doi: 10.1029/2017JC013624

Francis, J. A. (2017, 12). *Why are Arctic linkages to extreme weather still up in the air?* (Vol. 98) (No. 12). American Meteorological Society. Retrieved from http://journals.ametsoc.org/doi/10.1175/BAMS-D-17-0006.1 doi: 10.1175/BAMS-D-17-0006.1

Francis, J. A., Skific, N., & Vavrus, S. J. (2018, 10). North American Weather Regimes Are Becoming More Persistent: Is Arctic Amplification a Factor? *Geophysical Research Letters*, *45*(20), 414–11. Retrieved from https://onlinelibrary.wiley.com/doi/abs/10.1029/2018GL080252 doi: 10.1029/2018GL080252

Gao, Y., Sun, J., Li, F., He, S., Sandven, S., Yan, Q., ... Suo, L. (2015, 1). Arctic sea ice and Eurasian climate: A review. *Advances in Atmospheric Sciences*, *32*(1), 92–114. Retrieved from http://link.springer.com/10.1007/s00376

-014-0009-6 doi: 10.1007/s00376-014-0009-6

Gille, S. T. (2005, 9). Statistical Characterization of Zonal and Meridional Ocean Wind Stress. *Journal of Atmospheric and Oceanic Technology*, *22*(9), 1353–1372. Retrieved from http://journals.ametsoc.org/doi/abs/10.1175/JTECH1789.1 doi: 10.1175/JTECH1789.1

Haine, T. W., Curry, B., Gerdes, R., Hansen, E., Karcher, M., Lee, C., ... Woodgate, R. (2015, 2). *Arctic freshwater export: Status, mechanisms, and prospects* (Vol. 125). Elsevier. Retrieved from http://www.sciencedirect.com/science/article/pii/S0921818114003129 doi: 10.1016/j.gloplacha.2014.11.013

Holmes, R. M., McClelland, J. W., Peterson, B. J., Tank, S. E., Bulygina, E., Eglinton, T. I., ... Zimov, S. A. (2012, 3). Seasonal and Annual Fluxes of Nutrients and Organic Matter from Large Rivers to the Arctic Ocean and Surrounding Seas. *Estuaries and Coasts*, *35*(2), 369–382. Retrieved from http://link.springer.com/10.1007/s12237-011-9386-6 doi: 10.1007/s12237-011-9386-6

Lenn, Y. D., Wiles, P. J., Torres-Valdes, S., Abrahamsen, E. P., Rippeth, T. P., Simpson, J. H., ... Kirillov, S. (2009, 3). Vertical mixing at intermediate depths in the Arctic boundary current. *Geophysical Research Letters*, *36*(5), L05601. Retrieved from http://doi.wiley.com/10.1029/2008GL036792 doi: 10.1029/2008GL036792

Lincoln, B. J., Rippeth, T. P., Lenn, Y. D., Timmermans, M. L., Williams, W. J., & Bacon, S. (2016, 9). Wind-driven mixing at intermediate depths in an ice-free Arctic Ocean. *Geophysical Research Letters*, *43*(18), 9749–9756. Retrieved from http://doi.wiley.com/10.1002/2016GL070454 doi: 10.1002/2016GL070454

McDougall, T. J., & Barker, P. (2011). *Getting started with TEOS-10 and the Gibbs Seawater (GSW) Oceanographic Toolbox.* SCOR/IAPSO WG127.

Micklin, P. P. (1987). The Fate Of "Sibaral": Soviet Water Politics In The Gorbachev Era. *Central Asian Survey*, *6*(2), 67–88. doi: 10.1080/02634938708400585

Micklin, P. P. (1988). *Soviet River Diversion Projects: Problems and Prospects* (Tech. Rep.). Retrieved from https://www.ucis.pitt.edu/nceeer/

1988-0802-09-Micklin.pdf

Micklin, P. P. (2007, 5). The Aral Sea Disaster. *Annual Review of Earth and Planetary Sciences*, *35*(1), 47–72. Retrieved from http://www.annualreviews.org/doi/10.1146/annurev.earth.35.031306.140120 doi: 10.1146/annurev.earth.35.031306.140120

Micklin, P. P. (2011). The Siberian Water Transfer Scheme. In *Engineering earth* (pp. 1515–1530). Dordrecht: Springer Netherlands. Retrieved from http://www.springerlink.com/index/10.1007/978-90-481-9920-4_86 doi: 10.1007/978-90-481-9920-4{_}86

Nummelin, A., Li, C., & Smedsrud, L. H. (2015, 4). Response of Arctic Ocean stratification to changing river runoff in a column model. *Journal of Geophysical Research: Oceans*, *120*(4), 2655–2675. Retrieved from http://doi.wiley.com/10.1002/2014JC010571 doi: 10.1002/2014JC010571

Onarheim, I. H., Eldevik, T., Smedsrud, L. H., & Stroeve, J. C. (2018, 6). Seasonal and regional manifestation of Arctic sea ice loss. *Journal of Climate*, *31*(12), 4917–4932. Retrieved from http://journals.ametsoc.org/doi/10.1175/JCLI-D-17-0427.1 doi: 10.1175/JCLI-D-17-0427.1

Pearce, F. (2004). *Russia reviving massive river diversion plan.* Retrieved from https://www.newscientist.com/article/dn4637-russia-reviving-massive-river-diversion-plan/www.newscientist.com/article/dn4637

Pemberton, P., Nilsson, J., & Meier, H. E. M. (2014, 12). Arctic Ocean freshwater composition, pathways and transformations from a passive tracer simulation. *Tellus A: Dynamic Meteorology and Oceanography*, *66*(1), 23988. Retrieved from https://www.tandfonline.com/doi/full/10.3402/tellusa.v66.23988 doi: 10.3402/tellusa.v66.23988

Petoukhov, V., & Semenov, V. A. (2010, 11). A link between reduced Barents-Kara sea ice and cold winter extremes over northern continents. *Journal of Geophysical Research Atmospheres*, *115*(21), D21111. Retrieved from http://doi.wiley.com/10.1029/2009JD013568 doi: 10.1029/2009JD013568

Polyakov, I. V., Padman, L., Lenn, Y. D., Pnyushkov, A., Rember, R., & Ivanov, V. V. (2019, 1). Eastern arctic ocean diapycnal heat fluxes through large double-diffusive steps. *Journal of Physical Oceanography*, *49*(1), 227–246. Retrieved from http://journals.ametsoc.org/doi/10.1175/JPO-D-18-0080.1

553 doi: 10.1175/JPO-D-18-0080.1

554 Polyakov, I. V., Pnyushkov, A., & Carmack, E. (2018). Stability of the arctic halo-
555 cline: A new indicator of arctic climate change. *Environmental Research Let-*
556 *ters*, *13*. doi: 10.1088/1748-9326/aaec1e

557 Polyakov, I. V., Pnyushkov, A. V., Alkire, M. B., Ashik, I. M., Baumann, T. M.,
558 Carmack, E. C., ... Yulin, A. (2017, 4). Greater role for Atlantic inflows on
559 sea-ice loss in the Eurasian Basin of the Arctic Ocean. *Science (New York,*
560 *N.Y.)*, *356*(6335), 285–291. Retrieved from `http://www.ncbi.nlm.nih.gov/`
561 `pubmed/28386025` doi: 10.1126/science.aai8204

562 Polyakov, I. V., Pnyushkov, A. V., Rember, R., Padman, L., Carmack, E. C., &
563 Jackson, J. M. (2013, 10). Winter Convection Transports Atlantic Water
564 Heat to the Surface Layer in the Eastern Arctic Ocean. *Journal of Physical*
565 *Oceanography*, *43*(10), 2142–2155. Retrieved from `http://journals.ametsoc`
566 `.org/doi/abs/10.1175/JPO-D-12-0169.1` doi: 10.1175/JPO-D-12-0169.1

567 Rudels, B., Anderson, L. G., & Jones, E. P. (1996, 4). Formation and evolution
568 of the surface mixed layer and halocline of the Arctic Ocean. *Journal of Geo-*
569 *physical Research*, *101*(C4), 8807. Retrieved from `http://doi.wiley.com/10`
570 `.1029/96JC00143` doi: 10.1029/96JC00143

571 Rudels, B., Korhonen, M., Schauer, U., Pisarev, S., Rabe, B., & Wisotzki, A. (2015,
572 3). Circulation and transformation of Atlantic water in the Eurasian Basin
573 and the contribution of the Fram Strait inflow branch to the Arctic Ocean heat
574 budget. *Progress in Oceanography*, *132*, 128–152. Retrieved from `https://`
575 `www.sciencedirect.com/science/article/pii/S0079661114000494` doi:
576 10.1016/j.pocean.2014.04.003

577 Schauer, U., Fahrbach, E., Osterhus, S., & Rohardt, G. (2004). Arctic warm-
578 ing through the Fram Strait: Oceanic heat transport from 3 years of mea-
579 surements. *Journal of Geophysical Research: Oceans*, *109*(6), C06026.
580 Retrieved from `http://doi.wiley.com/10.1029/2003JC001823` doi:
581 10.1029/2003JC001823

582 Schmidtko, S., Johnson, G. C., & Lyman, J. M. (2013, 4). MIMOC: A global
583 monthly isopycnal upper-ocean climatology with mixed layers. *Jour-*
584 *nal of Geophysical Research: Oceans*, *118*(4), 1658–1672. Retrieved from
585 `http://doi.wiley.com/10.1002/jgrc.20122` doi: 10.1002/jgrc.20122

Screen, J. A., Deser, C., Smith, D. M., Zhang, X., Blackport, R., Kushner, P. J., ... Sun, L. (2018, 2). Consistency and discrepancy in the atmospheric response to Arctic sea-ice loss across climate models. *Nature Geoscience*, 1. Retrieved from http://www.nature.com/articles/s41561-018-0059-y doi: 10.1038/s41561-018-0059-y

Serreze, M. C., & Barry, R. G. (2011, 5). Processes and impacts of Arctic amplification: A research synthesis. *Global and Planetary Change*, *77*(1-2), 85–96. Retrieved from https://www-sciencedirect-com.ezproxy.bangor.ac.uk/science/article/pii/S0921818111000397 doi: 10.1016/J.GLOPLACHA.2011.03.004

Serreze, M. C., & Francis, J. (2006). The Arctic Amplification Debate. *Climatic Change*, *76*(3), 241–264. doi: 10.1007/s10584-005-9017-y

Sévellec, F., Fedorov, A. V., & Liu, W. (2017, 7). Arctic sea-ice decline weakens the Atlantic Meridional Overturning Circulation. *Nature Climate Change*, *7*(8), 604–610. Retrieved from http://www.nature.com/doifinder/10.1038/nclimate3353 doi: 10.1038/NCLIMATE3353

Shabad, T. (1983, 12). *Soviet, after studies, shelves plans to turn Siberian Rivers.*

Shibley, N. C., Timmermans, M. L., Carpenter, J. R., & Toole, J. M. (2017, 2). Spatial variability of the Arctic Ocean's double-diffusive staircase. *Journal of Geophysical Research: Oceans*, *122*(2), 980–994. Retrieved from http://doi.wiley.com/10.1002/2016JC012419 doi: 10.1002/2016JC012419

Simpson, J. H. (1981). The Shelf-Sea Fronts: Implications of their Existence and Behaviour. *Philosophical Transactions of the Royal Society of London. Series A, Mathematical and Physical Sciences*, *302*, 531–546. Retrieved from http://www.jstor.org/stable/37036 doi: 10.2307/37036

Simpson, J. H., & Sharples, J. (2012). *Introduction to the Physical and Biological Oceanography of Shelf Seas.* Cambridge, UK: Cambridge University Press.

Steele, M., & Boyd, T. (1998, 5). Retreat of the cold halocline layer in the Arctic Ocean. *Journal of Geophysical Research: Oceans*, *103*(C5), 10419–10435. Retrieved from http://doi.wiley.com/10.1029/98JC00580 doi: 10.1029/98JC00580

Stroeve, J., & Notz, D. (2018). Changing state of Arctic sea ice across all seasons. *Environmental Research Letters*, *13*(10), 103001.

Tang, Q., Zhang, X., Yang, X., & Francis, J. A. (2013, 3). Cold winter extremes in northern continents linked to Arctic sea ice loss. *Environmental Research Letters*, *8*(1), 014036. Retrieved from http://stacks.iop.org/1748-9326/8/i=1/a=014036?key=crossref.3b07e12952c5b61acb8cedc9b207e051 doi: 10.1088/1748-9326/8/1/014036

Turner, J. S. (2010, 1). The Melting of Ice in the Arctic Ocean: The Influence of Double-Diffusive Transport of Heat from Below. *Journal of Physical Oceanography*, *40*(1), 249–256. Retrieved from http://journals.ametsoc.org/doi/abs/10.1175/2009JPO4279.1 doi: 10.1175/2009JPO4279.1

Vihma, T. (2014, 9). Effects of Arctic Sea Ice Decline on Weather and Climate: A Review. *Surveys in Geophysics*, *35*(5), 1175–1214. Retrieved from http://link.springer.com/10.1007/s10712-014-9284-0 doi: 10.1007/s10712-014-9284-0

Wang, Y., Bi, H., Huang, H., Liu, Y., Liu, Y., Liang, X., ... Zhang, Z. (2019, 1). Satellite-observed trends in the Arctic sea ice concentration for the period 1979–2016. *Journal of Oceanology and Limnology*, *37*(1), 18–37. doi: 10.1007/s00343-019-7284-0

Yeager, S. G., & Large, W. G. (2008). *CORE.2 Global Air-Sea Flux Dataset.* Boulder, CO: Research Data Archive at the National Center for Atmospheric Research, Computational and Information Systems Laboratory. Retrieved from https://doi.org/10.5065/D6WH2N0S doi: 10.5065/D6WH2N0S

Zhang, P., Wu, Y., Simpson, I. R., Smith, K. L., Zhang, X., De, B., & Callaghan, P. (2018, 7). A stratospheric pathway linking a colder Siberia to Barents-Kara Sea sea ice loss. *Science Advances*, *4*(7), eaat6025. Retrieved from http://advances.sciencemag.org/lookup/doi/10.1126/sciadv.aat6025 doi: 10.1126/sciadv.aat6025

Zou, Y., Wang, Y., Zhang, Y., & Koo, J. H. (2017, 3). Arctic sea ice, Eurasia snow, and extreme winter haze in China. *Science Advances*, *3*(3), e1602751. Retrieved from http://advances.sciencemag.org/lookup/doi/10.1126/sciadv.1602751 doi: 10.1126/sciadv.1602751

Zygmuntowska, M., Rampal, P., Ivanova, N., & Smedsrud, L. H. (2014). Uncertainties in Arctic sea ice thickness and volume: new estimates and implications for trends. *The Cryosphere*, *8*, 705–720. Retrieved from

652 www.the-cryosphere.net/8/705/2014/ doi: 10.5194/tc-8-705-2014